Actinides in molecules : exotic properties probed by X-ray Absorption Spectroscopy

C. Den Auwer[1], P. Moisy[1], P. Guilbaud[1], D. Guillaumont[1], E. Simoni[2], S. D. Conradson[3]

[1]*CEA Marcoule DEN/DRCP/SCPS, 30207 Bagnols-sur-Cèze Cedex, France*
[2] *Université Paris Sud, IPN, 91405 Orsay Cedex, France*
[3] *Los Alamos Nat. Lab., MST Division, Los Alamos, NM 87545, USA*

Abstract – *Dealing with actinide elements in molecular chemistry may result in particularly attractive and exotic physico-chemical properties. In solution, one of the spectroscopic tools able to selectively probe the structural or electronic properties of these molecules is the X-ray absorption process. Different aspects of absorption edge or EXAFS analysis related to actinide studies are presented, including phenomenological and semi-quantitative approaches.*

INTRODUCTION

Due to their incomplete 5f and 6d electronic shells, the actinide elements present some unusual physical and chemical properties. Moreover, the actinide very large atomic numbers are also responsible for very important relativistic effects, among which the scalar effect is at the origin of the so-called lanthanidic and actinidic contraction. Another consequence is that the elements of the first half part of the actinide series exhibit a large number of stable or metastable formal oxidation states ranking from III to VII depending on the atomic number. Thus, the question of delocalized *vs* localized behavior of the 5f electrons still remains a critical issue to be addressed from both experimental and theoretical points of view. Oxidation states III and IV are formally spherically symmetric cations while oxidation sates V and VI have a transdioxo skeletons with coordination sites in the equatorial plane. Because most of the actinide complexes (from uranium to americium) with oxidation states higher than IV do contain the actinyl AnO_2^{n+} (n = 1, 2) moieties, there are of technological and environmental primary importance. Furthermore, the ubiquity of the uranyl cation in the geosphere, because of its remarkable stability, makes it one of the most extensively investigated cation within the actinide family. The major characteristic of actinyl cations is the occurrence of quasi linear O-An-O unit with a short An-O multiple bond and a bond length ranking from 1.7 to 1.9 Å depending on the cation. This characteristic is also specific of the actinide family as only one analogue (the osmyl cation OsO_2^{2+}) is known in the d block [1]. This is a good evidence of the bonding particularity that involves significant participation of the 5f orbitals in the HOMO of the AnO_2^{n+} unit. As a matter of fact, the bent structure of molecular ThO_2 versus the linear one of U, Np and Pu elements has been the subject of numerous theoretical works questioning the extent of the 5f and 6d participation in the bonding molecular orbitals involving the two oxygen atoms [2].

The use of X-ray Absorption Spectroscopy in the hard X-ray regime to investigate actinide molecular adducts has been of increasing interests in the past decade. This is particularly true for species in solutions, when complementary speciation techniques as optical and vibrational spectroscopies or quantum chemical investigation can be employed. Thus, the X-ray probe can be considered as a fingerprint of the structure of the cation polyhedron. Additionally, in the edge regime, electronic properties as valence orbital population and localization can be obtained.

MEASURING THE X RAY ABSORPTION

Although one of the major advantage of XAS is the ability to tune the absorption edge for a given element, most of the actinyl studies have dealt with L_{III} and more rarely L_I edges [3]. Reasons for this limitation are mainly technical because it allows measurement across multiple barrier confinement of the sample. General considerations related to the manipulation of radionuclides at the synchrotron sources have been summarized in the Proceeding of the 2nd Euroconference and NEA Workshop on Speciation, Techniques and Facilities for Radioactive Materials at Synchrotron Light Sources [4].

The X-ray absorption spectrum of a given element is commonly divided in two different regions, the pre-edge and edge region, called XANES, and the post-edge region, called EXAFS, which corresponds to significantly different processes. In the edge region, low energy excited states are considered and

transitions to bound states or quasi-bound states are often observed. In a simple one-electron molecular-orbital (MO) picture, the authorized LUMO or partially vacant valence orbitals are probed by the photoelectron according to the dipolar transition rule. Quadrupolar transition or phonon coupling can also contribute to the edge as observed for several transition metals. Within the one-electron multiple scattering picture, both absorption coefficient μ and l-projected density of states (DOS) ρ have smooth atomic backgrounds modulated by the oscillating function χ. Transitions to bound or quasi-bound states resulting from mixing with continuum states occur bellow or around the vacuum level. Above the continuum threshold, in the EXAFS regime, the final one-electron state belongs to the continuum and the spectrum is dominated by constructive or destructive interferences contained in χ.

ACTINIDE MOLECULAR CHEMISTRY

The molecular systems selected for this proceeding are formally divided in four parts from simple to complex molecular edifices : aquo form of the actinide and transition metal cations and more specifically UO_2^{2+}, NpO_2^{2+}, OsO_2^{2+}; reactivity of UO_2^{2+} upon uptake onto mineral surfaces; U, Np, Pu, Am involved in three-dimensional molecular building blocks; metalloprotein behavior upon uptake of U, Np radionuclides.

Learning from edge spectroscopy of aqueous species

Three of the four molecular structures considered here are solvent adducts: $[UO_2(H_2O)_5]^{2+}$, $[NpO_2(H_2O)_5]^{2+}$ and $[NpO_2(OH)_4]^{2-}$ [5]. In order to account for the solvent part beyond the first coordination sphere, an approach using molecular dynamic calculations has been performed for these systems in aqueous solution, leading to a sampling for both the first sphere hydrogen atoms and the surrounding water molecules around the actinyl rod. The fourth adduct $[OsO_2(OH)_4]^2$, selected here as a point of comparison with the actinide elements is insoluble in aqueous solutions. Figure 1 compares the experimental L_{III} edge of $[UO_2(H_2O)_5]^{2+}$ with 6 XANES calculations based on clusters obtained from 6 snapshots of the molecular dynamical calculation. Qualitatively, all the calculations reproduce the XANES features, *i.e.* the strong white line A, shoulder B

attributed to the multiple scattering contribution of the transdioxo unit and shoulder C (even if it is less intense in the simulation than in the experimental spectrum). Although some differences appear between each calculation corresponding to each snapshot, the broad character of the edge spectrum precludes the selection of one preferred conformation over another one by comparison with the experiment. The spectrum obtained when averaging the 6 calculations (which should represent the averaged conformation of the molecule in water) is indeed in very good agreement with the experiment. The geometry of $[OsO_2(H_2O)_5]^{2+}$ molecular skeleton exhibits a strong distortion compared to the ones of U and Np : an axial distance of 1.75 Å and very short equatorial distances of 2.03 Å. A clear signature of these structural changes is observed on Figure 1.
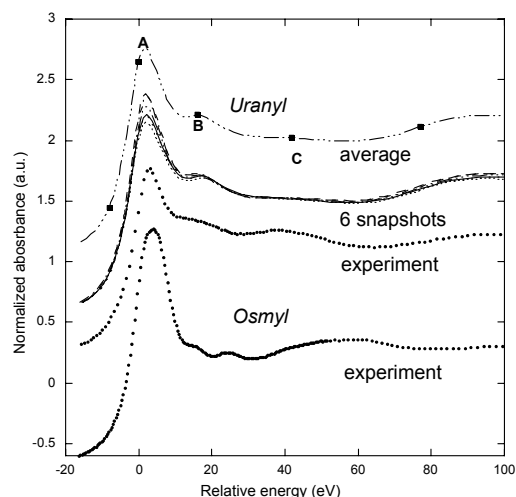

Fig. 1: Experimental and calculated (Feff8.2) L_{III} edge of $[UO_2(H_2O)_5]^{2+}$ and $[OsO_2(H_2O)_5]^{2+}$.

Figure 2 shows the L_{III} edges of neptunyl in both acidic ($[NpO_2(H_2O)_5]^{2+}$) and basic ($[NpO_2(OH)_4]^{2-}$) aqueous solutions. The structural distortion of the molecular skeleton from acidic to basic media corresponds to an elongation of 0.07 Å of the axial distances and a contraction of 0.21 Å of the equatorial distances. Comparison of the corresponding experimental L_{III} edges shows that this deformation leads to dramatic changes in the edge spectrum: strong differences in the intensity of A, shifts of B and C in the spectrum of $[NpO_2(H_2O)_5]^{2+}$ compared to $[NpO_2(OH)_4]^{2-}$. These differences are well reproduced by the calculation. A comparison with Figure 1 shows that the spectra of $[UO_2(H_2O)_5]^{2+}$ and $[NpO_2(H_2O)_5]^{2+}$ are very comparable due to the similarity of both

skeletons. The strong differences observed in the edge spectrum of $[NpO_2(OH)_4]^{2-}$ confirm that the geometry of the first coordination sphere plays a major role in the shape of the edge. As described for the uranium edge, the position of feature B with respect to A is indicative of the axial Np-O distance. In $[NpO_2(OH)_4]^{2-}$, B is shifted to lower energies compared to $[NpO_2(H_2O)_5]^{2+}$, in agreement with a larger axial distance for the hydroxide with respect to the hydrate. The identity of the product ΔER^2 is indeed verified within the measurement error: $\Delta ER^2 = 12.5(eV) \cdot 1.75(Å)^2 = 38$ for $[NpO_2(H_2O)_5]^{2+}$; $\Delta ER^2 = 10.0(eV) \cdot 1.82(Å)^2 = 33$ for $[NpO_2(OH)_4]^{2-}$. Conversely, a careful analysis of the edge shape and feature positions may lead to reliable structural information about the near structure around the actinide cation.
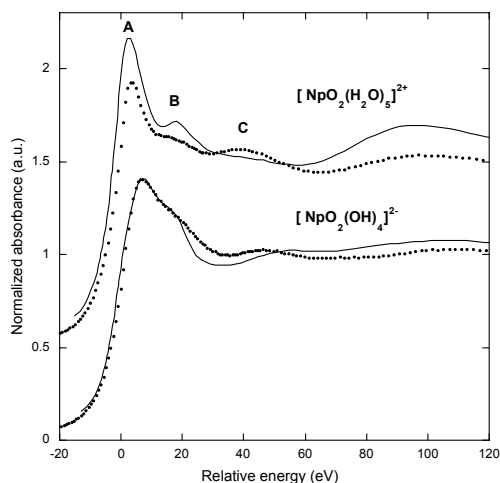

Fig. 2: Experimental (....) and calculated (-) (Feff8.2) L_{III} edge of $[NpO_2(H_2O)_5]^{2+}$ and $[NpO_2(OH)_4]^{2-}$.

Interaction with mineral surfaces

In order to model the interactions between heavy metal ions and mineral surfaces in aqueous medium, a detailed knowledge of the physico-chemical reactions at the solid-solution interface is required. These interfacial reactions depend mainly on several geochemical parameters such as pH, redox potential and ionic strength of the aqueous medium, the speciation of the metal ion and the surface properties of the substrates (acidity and surface sites density), which makes a quantitative description rather complicated. Nevertheless, the macroscopic thermodynamics do not give any accurate information about the elementary chemical reactions used to determine the equilibrium constants. Thus, it is necessary to

relate the expected surface complexes to the structure of the surface coordination complexes. Therefore, the stoichiometry of the chemical species involved in such processes should be deduced from molecular-scale information given by spectroscopic investigations. Among the questions that XAS has addressed are inner versus outer-sphere complexation, formation of polynuclear precipitates, and mono versus polydentate surface binding modes. Although one of the drawbacks of the technique is to average the signal over all the possible species, tentative site by site data analysis has been successfully undertaken. In Figure 3, examples of EXAFS spectra of $UO_2^{2+}/H_2O/substrate$ (substrate = $LaPO_4$, ZrP_2O_7 and TiO_2) surface complexes are presented [6].
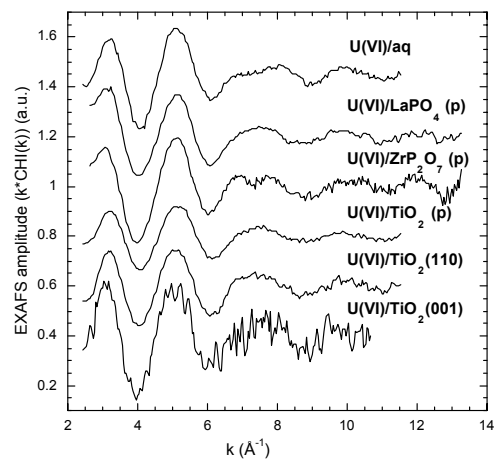

Fig. 3 : Experimental EXAFS L_{III} edge of uranyl sorbed onto mineral powders ($LaPO_4$, $ZrPO_4$, TiO_2) and mineral single crystal surfaces (TiO_2 plans (110) and (001)).

EXAFS data analysis of the uranyl sorbed onto the (110) plane shows a splitting of the equatorial U-O bond distances between U-O(surface) and U-O(out). Two possible sorption sites are available for bidentate complexation on the (110) surface : shared-edge distorted TiO_6 polyhedra and shared-summit polyhedra. Both sites are present in the surface complexes in proportions that are unknown from data analysis. Figure 4 shows a schematic representation of the surface complex in the case of the shared-edge sorption site of the (110) surface. The structural parameters are comparable to the one obtained from uranyl sorption on polycrystalline rutile. The shortening of the U-O equatorial bond from 2.42 Å for aqueous uranyl to 2.32 Å for U-O(surface) suggests an increase in covalency of the U-O(surface) bond. This would not be

surprising, taking into account the lack of coordination for the rutile surface oxygens and the possibility of charge delocalization along the surface.
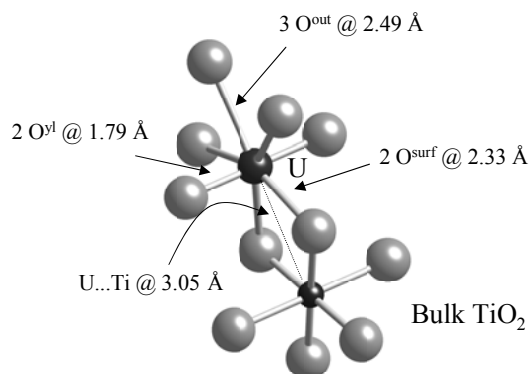

Fig. 4: Schematic representation of the uranyl complex upon sorption onto $TiO_2(110)$ crystal surface.

Towards more complex systems: the metalloprotein case.

Among the 18000 protein structures contained in the Protein Data Bank today, one-third are metalloproteins, i.e. chemical combinations of protein atoms with metallic cations such as iron, calcium, copper, zinc and magnesium for the most biological ones. When tightly bound to protein ligands, metal ions are critical to the function, structure, and stability of proteins, by only allowing specific interactions to take place and/or selective chemistry to occur. Metallobiomolecules are thus considered as elaborated inorganic complexes with well-designed metal active site structures. A protein-bound metal site consists of one or more metallic cations and all protein side chain and exogenous bridging and terminal ligands that define the first coordination sphere of each metal ion. Such metallic sites participate in the accomplishment of the most essential biological and chemical functions supported by proteins. Although the various interaction processes between the metallic cation and the protein have been widely studied in all the fields of biochemistry, focus on the specific actinide family is more seldom. In particular, the knowledge of transportation, fixation and interaction mechanisms of these cations in the biologically active sites are only partially understood.

Stable actinide cations at the formal oxidation state IV (Th, Np, Pu) but also oxocations are of first concern in case of contamination, for their ability to bind to proteic domains with great affinity and in particular transferrin. This protein is a glycoprotein made of 670 amino acids and is used as a regulator of Fe(III) carriage. Its tertiary structure is made of two equivalent lobes (C and N) with one possible complexation site each. The Fe coordination is in a distorted octahedral conformation with two coordinating tyrosines, one aspartate and one histidine (imidazole function). An additional synergetic anion (*in vivo*, carbonate) is positioned between the protein and the cation. Figure 5 shows the ovotransferrin tertiary structure with Fe(III) cation (PDB ref. 1NFT).
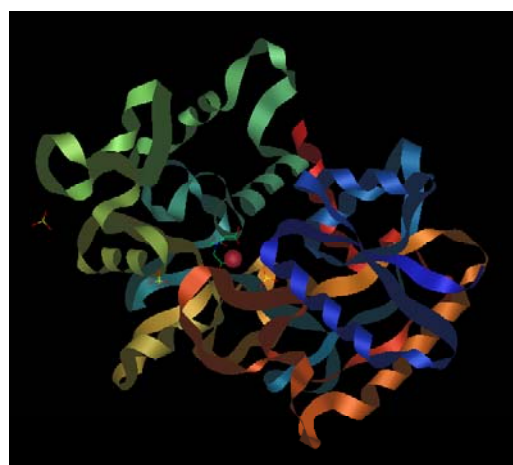

Fig. 5: tertiary structure of the Fe(IIII) ovotransferrin N-lobe complex.

First experimental results from Np(IV) complexation by human transferrin [7] in the presence of nitrosotriacetic acid (NTA) have been obtained at the Np L_{III} edge. A preliminary model assuming that the Np cation fills the Fe site of the protein has been attempted. It suggests that the cation is surrounded by one NTA chelate, two tyrosines from the protein and two water molecules. The average distance Np-ligand distance is 2.55 Å compared to 2.07 Å for the Fe case [8].

CONCLUSION

From speciation to simulation, XAS has proven to be one of the useful probe for actinide chemistry. Clearly the XAS probe by itself will not fully describe the electronic valence states of the molecule and a palette of complementary techniques and calculations must be employed. Also, limitation of XAS data analysis to phenomenological aspects is often restrictive and

coupling simulation codes to experimental results is essential. In that sense, the selection of various transition channels from core spectroscopy to higher primary quantum numbers is a unique tool based on the tunability of the synchrotron radiation.

REFERENCES

1. N. Kaltsoyannis, P. Scott, *The f elements*, Oxford Science Publisher, Zeneca (1999).
2. P. J. Hay, R. L. Martin, G. Schreckenbach, *J. Phys. Chem. A*, **104**, 6259 (2000).
3. C. Den Auwer, E. Simoni, S. D. Conradson, C. Madic, Eur. J. Inorg. Chem., **21**, 3843 (2003).
4. *Proc. of the Workshop on Speciation, Techniques and facilities for Radioactive Materials at Sunchrotron Light Sources*, OECD – NEA, 4 – 6 October, Grenoble, France (1998) and *Proc. 2nd Euroconference and NEA Workshop on Speciation, Techniques and Facilities for Radioactive Materials at Synchrotron Light Sources*, OECD – NEA, September, Grenoble, France (2001).
5. C. Den Auwer, D. Guillaumont, P. Guilbaud, S. D. Conradson, J. J. Rehr, A. Ankudinov, E. Simoni, *New J. Chem.* Accepted for publication.
6. C. Den Auwer, R. Drot, E. Simoni, S. D. Conradson, M. Gailhanou, J. Mustre de Leon, New J. Chem., **27**, 648 (2003).
7. R. Racine, Ph. Moisy, F. Paquet, H. Métivier, C. Madic, Radiochim. Acta, **91**, 115 (2003).
7. K. Mitzutani, H. Yamashita, H. Kurokawa, B. Mikami, M. Hirose, *J. Biol. Chem.*, **274**, 10190 (1999).